JCI The Journal of Clinical Investigation

Subdominance and poor intrinsic immunogenicity limit humoral immunity targeting influenza HA-stem

Hyon-Xhi Tan, … , Stephen J. Kent, Adam K. Wheatley

J Clin Invest. 2018. https://doi.org/10.1172/JCI123366.

Research In-Press Preview Immunology

Both natural influenza infection and current seasonal influenza vaccines primarily induce neutralising antibody responses against highly diverse epitopes within the “head” of the viral hemagglutinin (HA) protein. There is increasing interest on redirecting immunity towards the more conserved HA-stem or stalk as a means to broaden protective antibody responses. Here we examined HA-stem-specific B cell and T-follicular helper (Tfh) cell responses in the context of influenza infection and immunisation in mouse and monkey models. We found that during infection the stem domain was immunologically subdominant to the head in terms of serum antibody production and antigen-specific B and Tfh responses. Similarly, we found HA-stem immunogens were poorly immunogenic compared to the full-length HA with abolished sialic acid binding activity, with limiting Tfh elicitation a potential constraint to the induction or boosting of anti-stem immunity by vaccination. Finally, we confirm that currently licensed seasonal influenza vaccines can boost pre-existing memory responses against the HA-stem in humans. An increased understanding of the immune dynamics surrounding the HA-stem is essential to inform the design of next-generation influenza vaccines for broad and durable protection.

Subdominance and poor intrinsic immunogenicity limit humoral immunity targeting influenza HA-stem

Hyon-Xhi Tan[1]*, Sinthujan Jegaskanda[1]*, Jennifer A Juno[1]*, Robyn Esterbauer[1], Julius Wong[1], Hannah G Kelly[1], Yi Liu[1], Danielle Tilmanis[2], Aeron C Hurt[1, 2], Jonathan W Yewdell[3], Stephen J Kent[1, 4, 5]†, Adam K Wheatley[1]†.

[1]Department of Microbiology and Immunology, University of Melbourne, at The Peter Doherty Institute for Infection and Immunity, Melbourne, Victoria 3000, Australia.

[2] World Health Organization (WHO) Collaborating Centre for Reference and Research on Influenza, The Peter Doherty Institute for Infection and Immunity, Melbourne, Victoria 3000, Australia.

[3]Laboratory of Viral Diseases, National Institute of Allergy and Infectious Diseases, National Institutes of Health, Bethesda, Maryland, USA.

[4]Melbourne Sexual Health Centre and Department of Infectious Diseases, Alfred Hospital and Central Clinical School, Monash University, Melbourne, Victoria 3004, Australia.

[5]ARC Centre for Excellence in Convergent Bio-Nano Science and Technology, University of Melbourne, Parkville, Victoria 3010, Australia.

† Address correspondence to: a.wheatley@unimelb.edu.au / +61 3 9035 4179 (AKW); skent@unimelb.edu.au / +61 3 8344 9939 (SJK). Department of Microbiology and Immunology, University of Melbourne, at The Peter Doherty Institute for Infection and Immunity, Melbourne, Victoria 3000, Australia

Abstract

Both natural influenza infection and current seasonal influenza vaccines primarily induce neutralising antibody responses against highly diverse epitopes within the "head" of the viral hemagglutinin (HA) protein. There is increasing interest on redirecting immunity towards the more conserved HA-stem or stalk as a means to broaden protective antibody responses. Here we examined HA-stem-specific B cell and T-follicular helper (Tfh) cell responses in the context of influenza infection and immunisation in mouse and monkey models. We found that during infection the stem domain was immunologically subdominant to the head in terms of serum antibody production and antigen-specific B and Tfh responses. Similarly, we found HA-stem immunogens were poorly immunogenic compared to the full-length HA with abolished sialic acid binding activity, with limiting Tfh elicitation a potential constraint to the induction or boosting of anti-stem immunity by vaccination. Finally, we confirm that currently licensed seasonal influenza vaccines can boost pre-existing memory responses against the HA-stem in humans. An increased understanding of the immune dynamics surrounding the HA-stem is essential to inform the design of next-generation influenza vaccines for broad and durable protection.

Introduction

Influenza viruses cause significant global morbidity and mortality through seasonal epidemics and periodic pandemics. The effectiveness of influenza vaccination is limited by the focusing of humoral immunity on a cluster of highly mutable epitopes in the globular head domain of the viral hemagglutinin (HA). This results in neutralisation that is notoriously strain-specific and leaves human populations vulnerable to antigenically novel viruses arising via antigenic drift or emerging from zoonotic

52 reservoirs. Expanding vaccine immunity beyond classical, immunodominant variable
53 epitopes is critical for the development of more broadly effective vaccines.
54
55 HA epitopes in the conserved HA-stem have been identified that allow neutralisation
56 of highly diverse influenza strains by antibody (1-5). While targeting the stem has
57 energised efforts to develop universal influenza vaccines (6, 7), stem-specific
58 antibodies in humans are generally found at low serological concentrations (8), with
59 only limited increase after seasonal immunisation or infection (3, 9, 10). Infection or
60 immunisation with highly novel influenza viruses, for example the 2009 pandemic
61 H1N1 or avian H5N1, can drive the preferential expansion of stem-specific memory B
62 cells and serum antibody (10-12). However, subsequent re-exposure to matched HA re-
63 establishes humoral responses dominantly targeting the variable HA head domain (10,
64 13). The intrinsic immunological hierarchy that exists between the stem and head
65 regions of HA is further evident when site-directed glycosylation of the head domain
66 resulted in an 8-fold enhancement of stem-specific antibody titres relative to responses
67 induced by an unmodified HA counterpart (14). The immunological subdominance of
68 stem-specific B cell responses constitutes a major obstacle in efficiently targeting the
69 HA-stem by vaccination.
70
71 Despite extensive characterisation of humoral immunity to influenza spanning many
72 decades, the mechanisms driving establishment and maintenance of immunodominance
73 hierarchies to HA epitopes remain unclear. The polyspecificity (or self-reactivity) of
74 stem binding antibodies, particularly those derived from VH1-69 germlines, was
75 flagged as potentially reducing the responsiveness of stem-specific B cells in humans
76 (13). However, subdominance of stem responses is conserved in mice (15, 16) and
77 macaques (17), which lack human-like VH1-69 alleles, suggesting the importance of

78 other factors. Indeed, immunodominance of the HA globular head over the stem
79 extends to lampreys, which have evolved unique analogues to vertebrate antibodies
80 termed variable lymphocyte receptors (16). Andrews et al recently reported that stem
81 epitopes are poorly exposed on whole influenza virions relative to head epitopes,
82 constraining recognition by human antibodies (13) and potentially contributing to
83 immunological subdominance in vivo. These observations suggest that factors intrinsic
84 to the immunogens, such as protein conformation and epitope accessibility, may
85 underpin universal rules for B cell immunodominance hierarchies.
86
87 B cell intrinsic factors may also modulate antibody responses to HA. The frequency of
88 naïve precursors is known to contribute to immunodominance patterns in cytotoxic
89 CD8+ T cells responding to viral infection (18, 19). It remains possible that analogous
90 differences in naïve and/or memory B cell frequencies may contribute to stem versus
91 head immunodominance. However, the dynamics of polyclonal B cell selection to
92 complex antigens such as HA suggest precursor frequencies or initial B cell receptor
93 (BCR) avidities fail to explain positive selection within germinal centre responses or
94 contribution to serum antibody (20). Alternatively, qualitative differences may also be
95 critical; for instance, stem-specific B cells may be recruited less efficiently into nascent
96 immune responses, respond less robustly to antigenic stimuli or be impaired in the
97 ability to proliferate and/or terminally differentiate into plasma cells, which seed the
98 bone marrow and provide a lasting source of serum antibody. Finally, extrinsic factors
99 such as availability of T follicular helper (Tfh) cell responses may also be a limiting
100 factor in sufficiently stimulating robust proliferation of stem-specific B cells in active
101 germinal centres. Overall, a mix of immunogen intrinsic (concentration, localisation,
102 conformation of HA), B cell intrinsic (frequency, phenotype, proliferative capacity,

103 trafficking, polyspecificity) and extrinsic factors (CD4 T cell help) likely combine to
104 underpin the predominance of head versus stem humoral responses to influenza HA.
105
106 Here we demonstrate in naïve mouse and monkey models that immunological
107 subdominance of the HA-stem is established early during primary infection. In contrast
108 to head-specific responses, stem-specific B cells fail to expand, be recruited to
109 secondary lymphoid tissues or seed the plasma cell compartment in the bone marrow
110 following infection, despite high concentrations of HA-stem antigen at the site of
111 infection. Further, we show that HA-stem immunogens elicited poor stem-specific
112 responses in naïve or pre-immune animals, but that responses could be restored when
113 physically linked to either the head domain or a KLH (keyhole limpet haemocyanin)
114 carrier protein. Finally, we confirmed that currently licensed seasonal influenza
115 vaccines can drive re-expansion of stem-specific memory B cells and elevated stem-
116 specific serum antibody in humans. Greater mechanistic understanding of the drivers
117 of immunogenicity and immunodominance will inform vaccines strategies targeting
118 HA-stem epitopes as a pathway to universal influenza protection.

119 # Results

120 **Stem-specific B cell responses are highly subdominant during primary infection**
121 We first examined the spatial and temporal dynamics of HA and stem-specific humoral
122 immunity during primary H1N1 influenza infection in C57BL/6 mice intranasally
123 infected with A/Puerto Rico/8/1934 (PR8). To enable the study of HA specific
124 immunity, we first generated full-length HA (HA-FL) and stabilised HA-stem proteins
125 as described (6, 21), and confirmed antigenic specificity by binding to well
126 characterised monoclonal antibodies (Figure S1). After a single, non-lethal infection,
127 we observed the rapid development of a HA-FL specific serum antibody response by
128 day 7 (d7) post-infection, peaking at d28, and maintained at high titres out to d112

129 (Figure 1A). In contrast, serum antibody specific for the HA-stem was first detectable
130 only at d14 and then maintained at serum titres over 100-fold lower than antibodies to
131 HA-FL.
132
133 To directly assess influenza HA-FL and HA-stem specific immunity at the B cell level,
134 we examined the frequency and specificity of memory and germinal centre (GC) B cells
135 using PR8 HA-FL or PR8 HA-stem flow cytometry probes (gating Figure S2). Within
136 the mediastinal lymph node (MLN), which drains the lungs and where influenza-
137 specific B cell responses are initiated following infection (22-24), lymphoid
138 remodelling and GC responses were rapidly established (Figure S3). The HA-FL and
139 HA-stem probes allowed us to simultaneously track both total GC B cell responses
140 (B220+/IgD-/CD38lo/GL7+) and the proportions that were HA-FL or HA-stem-
141 specific. We found that both total GC B cells and the sizable subpopulation that were
142 HA-FL specific, expanded to d14 and were maintained at elevated levels until d112
143 (Figure 1B; representative plots Figure S4). During this time, B cell selection and
144 antibody affinity maturation to HA likely continues within the MLN (23). Within the
145 spleen, a major remodelling and significant GC expansion occurred post-infection
146 (Figure S5), with the frequency of HA-specific B cells within the GC population
147 reaching ~5% at d14, before waning over time. Neither GC formation or expansion of
148 HA-specific GC B cells was observed within the non-draining inguinal lymph node
149 (ILN).
150
151 HA-specific memory B cells (Bmem; B220+/IgD-/CD38hi/GL7-) peaked in the blood
152 at d14 before rapidly contracting to a stable ~0.3% of the total blood Bmem population
153 and maintained out to d112. Similar dynamics and resting frequencies were observed
154 within the memory populations in spleen and non-draining ILN. In contrast, HA-

155 specific MLN Bmem were rapidly expanded by d14 but maintained at high frequencies
156 (~2%) out to d112. Consistent with previous observations that the frequency of lymph
157 node B cells predict serum antibody immunodominance (15), our observations of low
158 serum antibody specific for the HA-stem coincided with very limited numbers of HA-
159 stem-specific B cells detected within the blood or lymphoid tissues by flow cytometry.
160 Similarly, while HA-specific B cells could be readily visualised by confocal
161 microscopy within the MLN (Figure S6) or spleen (Figure S7) of infected mice, we
162 could detect little to no staining for B cells binding the HA-stem either localised in GC
163 or distributed within the tissues.
164
165 To enumerate antigen-specific antibody-secreting cells (ASC) or plasma cells within
166 the bone marrow of infected mice, we devised an intracellular staining protocol of
167 CD138+ plasma cells with the HA-FL and HA-stem probes (Figure 1C; gating Figure
168 S8). In line with the low titres of stem antibodies, few stem-specific plasma cells were
169 evident, while plasma cells secreting antibody specific for HA-FL were readily
170 detected. The narrow epitope specificity of the PR8 HA-specific antibody and B cell
171 response was further confirmed using a HA probe derived from SV12 virus (15, 25),
172 which carries 12-amino acid substitutions enabling near total escape from serological
173 recognition at canonical epitopes (Figure S9). Thus, in line with previous studies (15),
174 primary PR8 infection in mice is dominated serologically and at the cellular level by B
175 cells that target canonical epitopes surrounding the receptor binding site, despite the
176 presence of bioavailable stem epitopes within the lungs of infected mice (Figure 1D).
177 Subdominance of the pandemic H1N1 (pdmH1N1) HA-stem was additionally
178 confirmed using A/California/04/2009 (CA09) infected mice (Figure S10). To confirm
179 that these observations were not exclusive to the C57BL/6 mouse strain, we examined

180 infected BALB/c mice and showed similar predominance of HA-FL over HA-stem
181 responses at d14 post-infection (Figure S11A and C).
182
183 To extend these findings to a more relevant animal model for human influenza, we
184 infected 8 pigtail macaques (*Macaca nemestrina*) with pdmH1N1 A/Auckland/1/2009,
185 which is antigenically indistinguishable from A/California/04/2009. Mean serum
186 endpoint levels at the peak of the response (d14 post-infection) were ~1:3800 and
187 ~1:600 for HA-FL and HA-stem responses, respectively (Figure 2A). While mean HA-
188 FL responses were maintained out to d56, HA-stem responses decreased 2-fold
189 (~1:300) relative to titres at d14. HA-stem responses were also 12-fold lower than HA-
190 FL responses at d56.
191
192 We examined the frequency of memory B cells (CD19+IgD-IgG+) in cryopreserved
193 peripheral blood mononuclear cell (PBMC) samples of infected macaques using CA09
194 HA-FL or HA-stem flow cytometry probes (Figure 2B). B cells specific for HA-FL
195 were detectable at day 14 (~0.1%), coinciding with the appearance of serological HA-
196 FL-specific antibodies, and slightly waned by d56. In contrast, little to no HA-stem-
197 specific B cells were detectable throughout the course of the pdmH1N1 infection. Both
198 murine and macaque infections displayed analogous kinetics in serology and blood-
199 circulating Bmem cells specific for HA-FL, which both peaked at d14, indicating that
200 infection models were similar.
201
202 Taken together, our data across mouse and macaque models show that the HA-stem is
203 markedly immunologically subdominant at both a cellular and serological level during
204 primary influenza infection in naïve animals.

205 **The HA-stem displays limited immunogenicity in isolation**

206 We next examined HA-specific humoral responses in the context of immunisation.
207 C57BL/6 mice were repeatedly immunised intramuscularly in the absence of adjuvant
208 with HA-FL, HA-stem or controls (PBS, phycoerythrin - PE). A steady increase in PE-
209 specific serum antibody was detected in PE-immunised mice (Figure 3A), with
210 boosting evident for three immunisations until a plateau was reached at a serum dilution
211 of ~1:10^5. Similarly, vaccination with HA-FL drove a steady increase in HA-FL serum
212 titres for all five immunisations, peaking at ~1:10^6 after the final boost. Sequential HA-
213 FL immunisation elicited serum antibody against the HA-stem at levels approximately
214 a log lower (peaking at ~1:10^5) than HA-FL serum titres. This observation indicates
215 that HA-FL immunisation partially overcomes stem subdominance. Interestingly,
216 repeated vaccination with HA-stem was comparatively poorly immunogenic, with stem
217 serum antibody not detectable until three immunisations, and peaking at titre of ~1:10^4.
218

219 Limited stem immunogenicity was maintained even when immunogens were
220 formulated with the adjuvant Addavax, an MF59 analogue. Two immunisations were
221 sufficient to elicit strong serum antibody responses (~1:10^6) for HA-FL or PE (Figure
222 3B). Analogous to the unadjuvanted regimen, stem-specific serum antibody was
223 detectable at high levels of ~1:10^6 when immunisations were performed with HA-FL
224 with Addavax. In contrast, only modest titres (~1:10^4) of stem serum antibody could be
225 elicited by two injections of HA-stem protein despite inclusion of adjuvant. We
226 repeated the HA-stem vaccinations with 4 additional adjuvants and via subcutaneous
227 immunisation but found that these regimens overall failed to rescue the HA-stem serum
228 antibody response (Figure S12). The poor immunogenicity of stem was relieved by
229 covalently coupling it to KLH. Immunisation with the conjugate in Addavax generated
230 a very high titre of stem-specific serum antibody response (Figure 3B) along with a
231 high KLH-specific serum antibody response (Figure S11B). While BALB/c mice

232 vaccinated with HA-FL in Addavax displayed similar immunological dominance of
233 HA-FL serum antibody responses, vaccination with the HA-stem immunogen in
234 Addavax elicited a stem-specific serum antibody response greater than that previously
235 seen in C57BL/6 mice (Figure S11B and C).
236
237 To further dissect limited HA-stem immunogenicity, we examined the recruitment of
238 stem-specific B cells into GC of draining ILN after a single immunisation with
239 Addavax-adjuvanted immunogens (Figure 3C and D). Mirroring the serum antibody
240 response, negligible GC recruitment of stem-specific B cells was observed with the
241 HA-stem protein alone, comparable to the PBS control. In contrast, immunisation with
242 the HA-FL protein or HA-stem with a KLH carrier induced strong GC recruitment of
243 stem-specific B cells. We further confirm that linkage to a nanoparticle scaffold (6)
244 relieved the poor immunogenicity of the HA-stem at both the serological and B cell
245 level (Figure S13). Taken together, these data suggest that the HA-stem domain in
246 isolation is intrinsically poorly immunogenic. However, strong stem-specific serum
247 antibodies and their corresponding GC B cells can be induced when the stem protein is
248 presented in the form of a full-length HA, when linked to a KLH carrier protein or when
249 displayed on the surface of a nanoparticle.

250 **The HA-stem elicits limited T follicular helper responses following vaccination**
251 **or infection**

252 Typical of protein antigens, CD4 T cells are required for robust and durable serum
253 antibody responses to HA (15, 26, 27). We therefore wondered whether the limited
254 immunogenicity of HA-stem immunogens is due to limiting Tfh responses. We
255 stimulated draining ILN T cells of immunised C57BL/6 mice with overlapping 17-mer
256 synthetic peptide sets encompassing the HA-head (residues HA1 42-313, H3
257 numbering) or HA-stem (HA1 0-42, 314-329, HA2 1-174) domains. Antigen-specific
258 Tfh (CD3+CD4+CXCR5++PD1++, Fig S14A) were detected based upon upregulation

259 of CD154 (CD40L, Fig S14B), a classical marker of CD4 T cell help, or the activation
260 induced markers OX40, CD25, and/or ICOS, which preferentially identify antigen-
261 specific Tfh cells compared to traditional intracellular cytokine staining (28-30) (Figure
262 S14C, D).
263
264 Ex vivo enumeration of ILN Tfh populations at day 14 post-immunisation confirmed
265 sizable Tfh populations could be recovered from both PR8 HA-FL and stem-KLH
266 immunised mice (Figure 4A). HA-FL immunisation induced significantly higher
267 levels of head-specific compared to stem-specific Tfh cells, irrespective of the surface
268 marker combinations used to define antigen-specific Tfh (p=0.005 for OX-
269 40++ICOS++ and OX-40++CD25+ responses, p=0.008 for CD154+ responses,
270 Figure 4B). Similar results were observed in BALB/c mice (Figure S15A).
271 Importantly, despite inducing stem-specific serum antibody and the expansion of Tfh
272 cells in the draining lymph nodes, stem-KLH vaccination did not elicit a stem-specific
273 Tfh response in C57BL/6 mice (Figure 4C) or in BALB/c mice (Figure S15B). We
274 confirmed, using either whole KLH protein or a subset of immunogenic KLH
275 peptides, that robust KLH-specific Tfh responses could be detected in stem-KLH
276 vaccinated animals (Figure S16). Together, these results suggest that deficient Tfh
277 elicitation may underpin the poor immunogenic potential of the stem-based
278 immunogen.
279
280 Extending these findings, we examined the frequency of HA head- and stem-specific
281 Tfh in the MLN of mice following intranasal PR8 infection. Consistent with the
282 immunisation data, HA-head-specific Tfh responses were readily detectible at day 14
283 post-infection, while stem-specific Tfh cells were rarely identified (Figure 4D),

284 suggesting that restricted Tfh responses targeting the HA-stem are independent of HA
285 antigen delivery modality.

286 **Selective recall of stem antibody responses is greatest in the context of HA-FL**
287 **immunisation**

288 We next examined the capacity of HA-stem immunogens to recall anti-stem antibody
289 responses in the context of pre-existing immunity, such as might be found in immune
290 adults. C57BL/6 mice were infected intranasally with PR8 before intramuscular
291 injection 56 days later with HA-FL and HA-stem immunogens. High serum antibody
292 titres to HA-FL could be detected post-infection in all animals, with a minor boosting
293 observed in groups immunised with HA-FL protein both with or without adjuvant
294 (Figure 5A). In line with the primary infection model, very low titres of stem-specific
295 serum antibody were observed post-infection. However, these stem-specific titres were
296 boosted following immunisation with HA-FL or HA-stem with a KLH carrier.
297 Interestingly, vaccination with the HA-stem immunogen alone, with or without
298 adjuvant, failed to elicit stem antibody responses in these pre-immune animals. This
299 was similarly evident when we examined recruitment of antigen-specific B cells into
300 the draining ILN, whereby HA-FL efficiently recruited both HA-FL- and stem-specific
301 B cells into GC following immunisation (Figure 5B). KLH-conjugated stem, but not
302 stem alone recruited stem-specific B cells into GC.
303

304 We next boosted six macaques experimentally infected with pdmH1N1 (from Figure
305 2A) with either 30 μg of HA-stem protein or a double dose (total 30 μg each HA) of
306 the seasonal quadrivalent inactivated influenza vaccine containing a pdmH1N1
307 component (IIV4; 2016 Fluarix Quad™). Consistent with the mouse model, IIV4
308 immunisation drove the efficient recall of HA-FL (3 of 3) and stem serum antibody
309 responses (2 of 3 animals) (Figure 5C), with a corresponding rise in serum
310 neutralisation titres as measured by focus reduction assay (Figure S17). In contrast,

311 immunisation with the HA-stem (using a conserved H1N1 HA-stem immunogen
312 derived from A/New Caledonia/20/1999 (6)), failed to recall HA-FL antibody, HA-
313 stem antibody or CA09 serum neutralisation activity. These patterns were recapitulated
314 when we examined the frequency of HA-FL- or HA-stem-specific B cells in the blood
315 of immunised macaques (Figure 5D), where a boosting of memory B cell frequencies
316 was observed only in animals receiving IIV4. Taken together, our results suggest that
317 the poor immunogenicity of HA-stem immunogens observed during primary
318 immunisation also translate into a diminished capacity to recall stem-specific memory
319 responses in pre-immune animals.

320 **Seasonal influenza vaccination of humans drives stem-specific antibody and**
321 **memory B cell expansion in humans**

322 There have been varying reports as to the degree to HA-stem responses are elicited by
323 seasonal immunisation in humans (3, 9, 10). Serological responses to seasonal vaccines
324 were assessed by ELISA in three cohorts of healthy Australian adult volunteers
325 receiving Southern Hemisphere formulations of 2015 IIV3 (Afluria™, N=29, (31)),
326 2016 IIV4 (FluQuadri™, N=18) or 2017 IIV4 (Afluria Quad™, N=21), which all
327 contained H1N1 A/California/06/2009 (2015 and 2016) or the antigenically similar
328 A/Michigan/45/2015 (2017). Serum antibody binding HA-FL or HA-stem was detected
329 within baseline samples in all subjects, with approximately 2-3-fold lower titres of
330 stem-specific antibody (Figure 6A). Significant expansion in endpoint titres of HA-FL
331 and HA-stem antibodies were observed following vaccine administration in all three
332 cohorts, but serological titres of stem-specific antibodies were consistently lower than
333 observed for HA-FL.

334

335 Although the use of recombinant trimeric HA probes for ex vivo identification of HA-
336 specific B cells by flow cytometry is well-established (2, 11, 21), stem-specific B cell
337 responses to seasonal influenza vaccines have not been extensively characterised. We

338 enumerated memory B cells recognising HA-FL or the HA-stem in seasonal vaccine
339 recipients. Cryopreserved PBMC samples from the IIV4 (2016) cohort were co-stained
340 with a B cell phenotyping panel (gating in Figure S18) and HA-FL or HA-stem probes,
341 with HA-specific B cell populations double stained to maximise specificity (Figure 6B).
342 Four weeks after immunisation, a significant expansion in memory B cell frequencies
343 from baseline was observed for both HA-FL and stem-specific populations (Figure 6C),
344 with the overall magnitude of memory B cell expansion similar for both populations
345 (Figure 6D). Similarly, using samples from the subsequent year cohort (IIV4 2017) and
346 co-staining with HA-FL and HA-stem probes (Figure 6E), we again observed a
347 significant and comparable expansion in HA-specific B cells binding both non-stem
348 and stem regions (Figure 6F, G). Indeed, a dramatic expansion of stem-specific memory
349 B cells could be directly observed in a subset of vaccine recipients (4 of 21) following
350 immunisation (Figure S19). To summarise, in subjects with pre-existing H1N1
351 influenza immunity, we confirm that stem responses are subdominant to head
352 responses, however seasonal influenza vaccines can drive expansion of HA-stem
353 specific humoral immunity. Thus, a general lack of stem-specific B cell responsiveness
354 does not seem to underpin the serological subdominance of stem-specific antibody
355 responses in humans.
356

357 **Discussion**

358 There is significant interest in universal influenza vaccination based on antibody
359 responses to the HA-stem. Consistent with previous reports (15, 16), we find that in
360 both mouse and monkeys, the HA-stem is subdominant to antibody responses targeting
361 canonical epitopes in the globular head domain. Stem-specific B cells fail to undergo
362 significant expansion, recruitment to germinal centres or differentiation into bone
363 marrow resident plasma cells following infection. The autoreactivity of human stem

364 antibodies was previously suggested as potential contributing factors to stem
365 subdominance (13). While autoreactivity or low naïve precursor frequencies would
366 likely inhibit recruitment of stem-specific B cells into a primary response, we found
367 that immunisation with recombinant HA-FL, HA-stem nanoparticles or HA-stem/KLH
368 conjugates could each induce high stem-specific serum antibody titres. Thus, any stem-
369 specific B cell defects are not absolute, and other factors must contribute to stem
370 subdominance.
371
372 The subdominance of the HA-stem might reflect an inability of stem-specific B cells to
373 interact with their cognate antigen *in vivo*. Steric hindrance of neutralising stem
374 epitopes in the context of whole influenza virions has been previously reported using
375 monoclonal antibodies (13). In the current study, we find that the HA-stem antigen is
376 widely prevalent at the site of infection. However, the extent and conformational
377 integrity of HA-stem antigens making it to the draining lymph nodes remains unclear.
378 Interestingly, we observed that HA-stem subdominance was greatest following virus
379 infection compared to soluble protein vaccination, suggesting that anchoring HA to
380 whole virions does limit B cell accessibility to the stem in vivo. Nevertheless, HA-stem
381 subdominance was still evident in the context of soluble protein immunisation where
382 these steric constraints are minimal.
383
384 Vaccines encompassing "headless" or "stabilised" HA-stem domains have been
385 developed and shown protection from influenza virus challenge in naïve animal models
386 (6, 7, 32-36). Here, we found repeated immunisation of C57BL/6 mice with a stable,
387 trimeric HA-stem immunogen either alone or with adjuvant, elicited markedly reduced
388 serum antibody responses compared with HA-FL, or a control phycoerythrin protein.
389 While the HA-FL immunogen used in this study carried a mutation abolishing binding

390 to cell surface sialic acids (21), we find the immunogenicity of the HA protein was not
391 markedly compromised by this change and was broadly comparable to the PE control.
392 Indeed, greater stem-specific serum antibody was detected in mice immunised with
393 HA-FL compared to the HA-stem in isolation, suggesting that the impact of the HA-FL
394 Y98F mutation on stem responses was minimal. In contrast to the HA-stem used in this
395 study, several previously designed HA-stem constructs have shown robust
396 immunogenicity and protection in vivo, despite some variants displaying
397 conformational misfolding (7, 33, 34, 36). Although a comprehensive head-to-head
398 comparison is difficult, these varied reports suggest that any immunogenicity defects
399 identified in the present study are not absolute and are heavily influenced by
400 immunogen design, particularly with substitutions in segments of the HA protein
401 retained, and the animal system used to evaluate stem vaccines. Indeed, we find
402 utilisation of a different mouse strain in the current study mounted better HA-stem
403 immunity compared to the C57BL/6 mouse model. Nevertheless, after infection or
404 immunisation in all animal models, we see consistently poorer humoral responses
405 targeting the HA-stem in comparison to HA-FL. The poor immunogenicity of the HA-
406 stem was associated with an inability to efficiently elicit CD4 help in vivo, with
407 maximal humoral responses rescued by conjugation to the HA head domain or KLH,
408 both of which successfully induced a Tfh response.
409
410 Diminished stem-specific Tfh was similarly observed during infection, suggesting that
411 the HA-stem could conceivably be lacking in MHC class II restricted T cell epitopes
412 relative to the globular head. Although a poor stem-specific Tfh response cannot fully
413 explain the subdominance of the stem during infection or in response to vaccination in
414 outbred populations, the murine data presented suggests that the magnitude of the Tfh
415 response could be a limiting factor in determining stem immunogenicity. Consequently,

416 the ability of the immunising antigen to elicit CD4+ T cell help in the context of diverse
417 MHC class II alleles should be an important consideration in the design of stem-based
418 universal influenza vaccines. Intriguingly, while immunodominance of HA-FL over
419 HA-stem was clearly observed in infected or vaccinated BALB/c mice carrying distinct
420 MHC-II alleles, we found HA-stem vaccination could elicit greater stem-specific
421 antibody responses than what was observed in C57BL/6 mice. In silico epitope analysis
422 predicted two putative epitopes of the HA-stem domain restricted by the MHC-II
423 molecule in BALB/c mice, while none were predicted for C57BL/6 mice (data not
424 shown), suggesting differences in HA-stem immunogenicity across these mouse strains
425 may be modulated by the availability of epitopes presented by MHC-II molecules and
426 the resulting Tfh response induced. It is also possible that the HA-stem and head
427 domains could be differentially susceptible to proteolytic degradation in vivo, which
428 may impact direct recognition by B cells as well as limiting peptide substrate
429 presentable to T cells. While we observed both HA head and HA-stem epitopes are
430 bioavailable in the lung following infection, the integrity and conformational state of
431 HA as presented to B cells in vivo is not known. Further studies are required to
432 accurately characterise the nature of HA localised within the relevant lymph nodes
433 following infection and immunisation.
434
435 Stem based universal vaccines need not induce primary B cell responses and instead
436 could target pre-existing immunological memory, which in humans originates from
437 near ubiquitous childhood infection (37, 38). Using infection in mice to establish
438 baseline immunity, we found that HA-stem immunogens, even in the presence of an
439 adjuvant, poorly recalled stem memory responses. By contrast, boosting with the HA-
440 FL or KLH-conjugated stem immunogens effectively recalled stem serum antibody.
441 Similarly, we observed poor recall of the stem response by the HA-stem immunogen in

442 macaques with pre-existing immunity, while IIV4 vaccination (analogous to HA-FL)
443 showed boosting of stem responses. However, our study does not exclude the
444 possibility of enhancing the HA-stem immunisation when formulated with other
445 adjuvant modalities in macaques. These observations suggest the poor elicitation of Tfh
446 observed during primary immunisation and infection might similarly constrain the
447 capacity of stem immunogens to recall immune memory.
448
449 HA-stem-specific memory B cells have been widely reported in adult humans (10, 11,
450 39) and were similarly evident within our cohorts. Following immunisation with
451 seasonal inactivated influenza vaccines, we observed a consistent expansion of stem-
452 specific immunity at a serological and B cell level, albeit to a lesser magnitude than
453 non-stem localised epitopes, broadly consistent with previous reports (3, 10). While
454 stem-specific memory B cells are clearly targetable by vaccination in humans and in
455 pre-immune animal models, the longevity of such responses remains unclear, with
456 suggestions that only stem immunity elicited by infection is long-lived (9). Further
457 studies into strategies to extend the durability of stem-specific immunity are warranted.
458
459 In summary, we find the immunological dynamics of humoral immunity targeting the
460 HA-stem domain are complex and context dependent. Our results suggest fundamental
461 constraints exist to limit the immunogenicity of the HA-stem domain during both
462 infection and immunisation, a finding consistent with the broad evolutionarily-
463 conserved immunological subdominance of this region. We cannot rule out that
464 different HA-stem directed vaccine approaches may have differing immunogenic
465 potential, given the diverse range of immunogen designs, expression systems,
466 formulations, immunisation schedules and animal models described (40). It does seem
467 likely, however, that boosting immunogenicity of the HA-stem via novel adjuvants,

468 carrier proteins or nanoparticle formulations will be necessary to elicit robust titres of
469 stem immunity in humans. Alternatively, strategies that maintain the coupling of head
470 and stem domains might be favourable (41, 42). A greater mechanistic understanding
471 of the molecular basis of immunogenicity, and how HA immunodominance hierarchies
472 are established and maintained, is required to guide the design of improved vaccination
473 regimes for broad protection against seasonal and emergent influenza viruses.

474 Methods

475 Seasonal IIV3 and IIV4 Clinical Samples

476 The 2015 IIV3 immunisation trial is fully described elsewhere (31) and registered as
477 NCT02632578 (http://www.clinicaltrials.gov). Briefly, 30 healthy Australian adults
478 were vaccinated with the 2015 Fluvax® (bioCSL) containing 15 μg of hemagglutinin
479 from A/California/07/2009-like (pdmH1N1), A/Switzerland/9715293/2013 (H3N2)-
480 like and B/Phuket/3073/2013-like strains. For the 2016 IIV4 trial 20 healthy adults were
481 administered FluQuadri® vaccine (Sanofi) containing A/California/07/2009-like virus
482 (pdmH1N1), A/Hong Kong/4801/2014-like virus (H3N2), B/Phuket/3073/2013-like
483 virus and B/Brisbane/60/2008-like virus components. For the 2017 IIV4 trial 22 healthy
484 adults were administered Afluria Quad® (Seqirus) vaccine containing
485 A/Michigan/45/2015 (pdmH1N1), A/Hong Kong/4801/2014-like virus (H3N2),
486 B/Phuket/3073/2013-like virus and B/Brisbane/60/2008-like virus components. For all
487 trials, sera, plasma and PBMCs were collected and cryopreserved at baseline (d0) and
488 day 28.

489 Animal infection and immunisation

490 All animal procedures were approved by the University of Melbourne Animal Ethics
491 Committee. For murine trials, C57BL/6 or BALB/c mice at 6-8 weeks of age were used.
492 Mice were anaesthetised by isoflurane inhalation prior to infection or immunisation.
493 For intranasal infections, mice were instilled with 50 μL volume of 50 $TCID_{50}$ or 500

494 $TCID_{50}$ doses for A/Puerto Rico/8/34 (PR8) or A/California/04/2009, respectively. For
495 vaccination studies, proteins were formulated at 5 μg HA or HA equivalent (stem-KLH)
496 diluted in PBS with or without adjuvant (1:1 Addavax, Invivogen; 1:1 R848, Invivogen;
497 1:4 CpG ODN 1826, Invivogen; 1:1 Complete/incomplete Freund's adjuvant, Sigma;
498 1:1 Sigma Adjuvant System, Sigma). Vaccinations were administered intramuscularly
499 via both hind quadriceps or subcutaneously via the abdomen.
500
501 Eight influenza-naive juvenile pigtail macaques (*Macaca nemestrina*) were studied as
502 approved by the Commonwealth Scientific and Industrial Research Organisation
503 Animal Health Animal Ethics Committee. Prior to any procedure, the animals were
504 anesthetised intramuscularly with ketamine. Macaques were inoculated with $1x10^7$ pfu
505 of A/Auckland/1/2009 via the larynx and tonsils as previously described (17) and serial
506 blood samples were subsequently obtained, with PBMC and serum cryopreserved.
507 Animals were immunised into both hind quadriceps with two doses of the 2016
508 Southern hemisphere IIV4 vaccines (GSKL Fluarix Tetra) or alternatively 30 μg of a
509 H1N1 stabilised stem protein derived from A/New Caledonia/20/1999 (6).

510 **HA proteins**

511 Recombinant HA-FL proteins used in immunisations, ELISA and flow cytometry
512 assays were derived for A/Puerto Rico/8/1934, A/California/7/2009, and
513 A/Michigan/45/2015 as previously described (21). HA-FL proteins carry a Y98F
514 mutation in the receptor binding site, which abolishes binding to cell surface sialic
515 acids. Stabilised HA-stem proteins were engineered for A/Puerto Rico/08/1934, A/New
516 Caledonia/20/1999 and A/California/7/2009 using methods established previously for
517 the design of Gen6 HA-stem in Yassine et al (6). Briefly, expression constructs were
518 synthesised (GeneArt) and cloned into mammalian expression vectors. HA-FL and HA-
519 stem proteins were expressed by transient transfection of Expi293 (Life Technologies)

520 suspension cultures and purified by polyhistadine-tag affinity chromatography and gel
521 filtration. Proteins were biotinylated using BirA (Avidity) and stored at -80°C. Prior to
522 use, biotinylated HA proteins were labelled by the sequential addition of streptavidin
523 (SA) conjugated to phycoerythrin (PE), allophycocyanin (APC) or BV421 and stored
524 at 4°C.

525 **Flow cytometric detection of HA-specific B cells**

526 HA-specific B cells were identified within cryopreserved human PBMC by co-staining
527 with HA probes conjugated to SA-PE, SA-APC, SA-BV421 or SA-Ax488. Cells were
528 stained with Aqua viability dye (Thermofisher). Monoclonal antibodies for surface
529 staining included: CD19-ECD (J3-119) (Beckman Coulter), CD20 Alexa700 (2H7),
530 IgM-BUV395 (G20-127), CD21-BUV737 (B-ly4), IgD-Cy7PE (IA6-2), IgG-BV786
531 (G18-145) (BD), CD14-BV510 (M5E2), CD3-BV510 (OKT3), CD8a-BV510 (RPA-
532 T8), CD16-BV510 (3G8), CD10-BV510 (HI10a), CD27-BV605 (O323) (Biolegend).
533 Background B cells interacting with SA were excluded by staining with SA-BV510
534 (BD). For macaque samples, PBMC were similarly stained with HA probes and the
535 human surface panel with the following alterations: IgD-Alexa488 (poly, Southern
536 Biotech), CD45 PE-Cy7 (D058-1283), CD20 BUV737 (2H7). For murine samples,
537 tissues were mechanically homogenised into single cell suspensions in RF10 media
538 (RPMI 1640, 10% FCS, 1× penicillin-streptomycin-glutamine; Life Technologies). For
539 bone marrow samples, cells were recovered by perfusion of both femurs with RF10.
540 Red blood cell lysis was performed with Pharm Lyse™ (BD). Isolated cells were
541 stained with Aqua viability dye (Thermofisher) and Fc-blocked with a CD16/32
542 antibody (93; Biolegend). Cells were then surface stained with the relevant HA-probes
543 and the following antibodies: B220 BUV737 (RA3-6B2; BD), IgD BUV395 (11-
544 26c.2a; BD), CD45 Cy7APC (30-F11; BD), GL7 Alexa488 (GL7; Biolegend), CD38
545 Cy7PE (90; Biolegend), Streptavidin BV786 (BD), CD3 BV786 (145-2C11;

546 Biolegend) and F4/80 BV786 (BM; Biolegend). Bone marrow samples were surface
547 stained with the aforementioned panel and CD138 BB515 (MI-15; BD) and CD138
548 BV711 (MI-15; BD), and stained intracellularly with HA-probes following fixation and
549 permeabilization. Cells were washed twice, fixed with 1% formaldehyde
550 (Polysciences) and acquired on a BD LSR Fortessa using BD FACS Diva.

551 **Flow cytometric detection of antigen-specific Tfh**

552 For ex vivo Tfh quantification, freshly isolated ILN single cell suspensions were
553 stained with the following antibodies: Live/dead Red (Life Technologies), CD3
554 BV510 (145-2C11; Biolegend), PD-1 BV786 (29F.1A12; Biolegend), CXCR5
555 BV421 (L138D7; Biolegend), CD4 BUV737 (RM4-5; BD), ICOS PerCP-eFluor710
556 (15F9; Life Technologies), B220 BV605 (RA3-6B2; BD), and F4/80 PE-Dazzle 594
557 (T45-2342; BD). To identify antigen-specific Tfh cells, freshly isolated ILN, MLN or
558 spleen samples were cultured in RF10 media for 18 hours at 37°C. Samples were
559 stimulated with a peptide pool (2 μg/peptide/mL) comprising the HA head (50
560 peptides) or HA stem domain (32 peptides), or a DMSO control. Peptide pools were
561 generated from a PR8 HA peptide array (17mers overlapping by 11 amino acids, BEI
562 resources) resuspended in DMSO. To identify KLH-specific Tfh cells, immunogenic
563 15mer peptides were predicted by Tepitool (http://tools.iedb.org/tepitool/, Immune
564 Epitope Database and Analysis Resource). The 20 most immunogenic peptide
565 predictions were synthesized (GenScript) and pooled for use in the Tfh assay. In some
566 cases, cells were stimulated with 5 μg/mL of whole protein (BSA or KLH). To
567 facilitate protein processing, lymph node suspensions labelled with CellTrace yellow
568 dye were co-cultured with splenocytes at a 10:1 ratio. At the time of stimulation, an
569 anti-CD154 BV650 or APC mAb (MR1; Biolegend and BD) was added to all culture
570 conditions. After stimulation, cells were washed twice in PBS and stained with Red
571 viability dye (Life Technologies) according to the manufacturer's instructions. Cells

572 were then stained with CD3 BV510 (145-2C11; Biolegend), CD25 BB515 (PD61;
573 BD), PD-1 BV786 (29F.1A12; Biolegend), CXCR5 BV421 (L138D7; Biolegend),
574 CD4 BUV737 (RM4-5; BD), OX-40 PeCy7 (OX-86; Biolegend), ICOS PerCP-
575 eFluor710 (15F9; Life Technologies), B220 BV605 (RA3-6B2; BD), and F4/80 PE-
576 Dazzle 594 (T45-2342; BD) before being washed, fixed and acquired on a BD LSR
577 Fortessa using BD FACS Diva.

578 **ELISA**

579 Antibody binding to HA-FL or HA-stem proteins was tested by ELISA. For human
580 samples, 96-well Immunosorp plates (Thermo Fisher) were coated overnight at 4°C
581 with 2 μg/mL recombinant HA proteins. After blocking with 1% FCS in PBS, duplicate
582 wells of serially diluted serum were added and incubated for two hours at room
583 temperature. Plates were washed prior to incubation with 1:30000 dilution of HRP-
584 conjugated anti-human IgG (Sigma) for 1 hour at room temperature. For macaque
585 samples, plates were coated overnight at 4°C with 2 μg/mL recombinant HA proteins
586 and blocked with 5% BSA in PBS. Duplicate wells of serially diluted serum were added
587 and incubated for two hours at room temperature. Plates were washed prior to
588 incubation with 1:10000 dilution of HRP-conjugated anti-monkey IgG (Rockland) for
589 1 hour at room temperature. For mouse samples, plates were coated overnight at 4°C
590 with 2 μg/mL recombinant HA proteins and blocked with 5% BSA in PBS. Duplicate
591 wells of serially diluted serum were added and incubated for two hours at room
592 temperature. Plates were washed prior to incubation with 1:10000 dilution of HRP-
593 conjugated anti-mouse IgG (KPL) for 1 hour at room temperature. In all cases, plates
594 were washed and developed using TMB substrate (Sigma) and read at 450nm. Endpoint
595 titres were calculated as the reciprocal serum dilution giving signal 2x background
596 using a fitted curve (4 parameter log regression).

597 **Confocal microscopy**

598 Fresh tissues were snap-frozen in O.C.T. compound (Sakura Finetek USA) and stored
599 at -80 °C. Tissues were sectioned at 7 µm thickness (Leica). Prior to staining, sectioned
600 tissues fixed in cold acetone solution (Sigma) for 10 min. Tissues were rehydrated with
601 PBS for 10 min and blocked with 5% (w/v) bovine serum albumin (Sigma) and 2%
602 (v/v) normal goat serum (NGS). To eliminate background signal of streptavidin-probes,
603 endogenous biotin was blocked using a streptavidin/biotin kit as per manufacturer's
604 protocol (Life Technologies).

605

606 For in situ staining of influenza-specific B cells, tissues were incubated with 2 µg/mL
607 of HA-probe conjugated to PE. To amplify the PE signal, tissues were stained
608 sequentially with rabbit polyclonal anti-PE antibodies (Novus Biologicals) and a
609 secondary goat anti-rabbit IgG Alexa Fluor 555 antibody (Life Technologies).
610 Influenza antigen staining in lungs was performed with 10 µg/mL of following
611 monoclonal antibodies: 441D6 (anti-HA head; provided by Dr Masaru Kanekiyo from
612 the Vaccine Research Center, NIAID, MD, USA), CR9114 (anti-HA stem), C179 (anti-
613 HA stem), D1-11 (anti-NP) and VRC01 (non-influenza control). Monoclonal
614 antibodies CR9114 (1), C179 (43), D1-11 (44) and VRC01 (45) were generated in-
615 house using publicly available sequences. Monoclonal antibody binding was
616 subsequently detected with a secondary goat anti-human IgG Alexa Fluor 555 antibody
617 (Life Technologies). Cell staining was performed using the following antibodies: B220
618 (RA3-6B2; BD), GL7 (GL7; Biolegend) and CD35 (8C12; BD). Slides were sealed
619 with ProLong Diamond Antifade Mountant (Life Technologies). Tiled images were
620 captured on a Zeiss LSM710 instrument. Post-processing of confocal images was
621 performed with ImageJ v2.0.0.

622 **Focus Reduction Assay**

623 Neutralisation activity of infected macaque sera was assessed against
624 A/Auckland/1/2009 using focus reduction assays as previously described (46). The
625 neutralisation titre is expressed as the reciprocal of the highest serum dilution at which
626 virus infection is inhibited by ≥ 50%.

627 **Statistical Analyses**

628 Data is generally presented as median +/- interquartile range or mean +/- SEM, as
629 indicated. Statistical significance was assessed by Mann-Whitney U or Wilcoxon
630 matched-pairs tests, as indicated. All tests were 2-tailed and a P value less than 0.05
631 was considered significant. Curve fitting was performed using 4 parameter logistic
632 regression. Flow data was analysed in FlowJo v9/10 and all statistical analyses were
633 performed using Prism (GraphPad).

634 **Study Approval**

635 The study protocols were approved by both the Alfred Hospital Ethics Committee (#
636 432/14), and the University of Melbourne Human Research Ethics Committee (#
637 1443420) and all associated procedures were carried out in accordance with the
638 approved guidelines. All participants provided written informed consent in accordance
639 with the Declaration of Helsinki. Animal studies and related experimental procedures
640 were approved by the University of Melbourne Animal Ethics Committee (#1714193).

641 # Competing interests

642 The authors declare no competing interests.

643 # Authors' contributions

644 HT, SJ, JAJ, SJK and AKW designed the study. HT, SJ, JAJ, RE, YL, JW, HGK, SJK
645 and AKW performed experiments. JWY provided key reagents. DT and ACH
646 performed serological and virological analyses. HT, JAJ, SJK and AKW wrote the
647 manuscript. All authors read and revised the manuscript.

648

649 # Acknowledgements

650 We thank all clinical trial staff and participants and Kathleen Wragg for technical
651 support. This work was supported by NHMRC program grant ID1052979 (SJK) and
652 NHMRC project grant ID1129099 (AKW). YL and JW are supported by a Melbourne
653 International Research Scholarship and Melbourne International Fee Remission
654 Scholarship. JAJ is supported by a NHMRC fellowship. The Melbourne World Health
655 Organization (WHO) Collaborating Centre for Reference Research on Influenza is
656 supported by the Australian Government Department of Health.

657 # References

658

659 1. Dreyfus C, Laursen NS, Kwaks T, Zuijdgeest D, Khayat R, Ekiert DC, et al.
660 Highly conserved protective epitopes on influenza B viruses. *Science.*
661 2012;337(6100):1343-8.
662 2. Joyce MG, Wheatley AK, Thomas PV, Chuang GY, Soto C, Bailer RT, et al.
663 Vaccine-Induced Antibodies that Neutralize Group 1 and Group 2 Influenza A
664 Viruses. *Cell.* 2016;166(3):609-23.
665 3. Corti D, Suguitan AL, Pinna D, Silacci C, Fernandez-Rodriguez BM, Vanzetta
666 F, et al. Heterosubtypic neutralizing antibodies are produced by individuals
667 immunized with a seasonal influenza vaccine. *The Journal of clinical*
668 *investigation.* 2010;120(5):1663-73.
669 4. Corti D, Voss J, Gamblin SJ, Codoni G, Macagno A, Jarrossay D, et al. A
670 neutralizing antibody selected from plasma cells that binds to group 1 and group
671 2 influenza A hemagglutinins. *Science (New York, NY).* 2011;333(6044):850-6.
672 5. Ekiert DC, Friesen RH, Bhabha G, Kwaks T, Jongeneelen M, Yu W, et al. A
673 highly conserved neutralizing epitope on group 2 influenza A viruses. *Science.*
674 2011;333(6044):843-50.
675 6. Yassine HM, Boyington JC, McTamney PM, Wei C-JJ, Kanekiyo M, Kong W-
676 PP, et al. Hemagglutinin-stem nanoparticles generate heterosubtypic influenza
677 protection. *Nature medicine.* 2015;21(9):1065-70.
678 7. Impagliazzo A, Milder F, Kuipers H, Wagner M, Zhu X, Hoffman RM, et al. A
679 stable trimeric influenza hemagglutinin stem as a broadly protective
680 immunogen. *Science.* 2015;349(6254):1301-6.
681 8. Sui J, Sheehan J, Hwang WC, Bankston LA, Burchett SK, Huang C-YY, et al.
682 Wide prevalence of heterosubtypic broadly neutralizing human anti-influenza
683 A antibodies. *Clinical infectious diseases : an official publication of the*
684 *Infectious Diseases Society of America.* 2011;52(8):1003-9.
685 9. Margine I, Hai R, Albrecht RA, Obermoser G, Harrod AC, Banchereau J, et al.
686 H3N2 influenza virus infection induces broadly reactive hemagglutinin stalk
687 antibodies in humans and mice. *Journal of virology.* 2013;87(8):4728-37.

688 10. Ellebedy AH, Krammer F, Li G-MM, Miller MS, Chiu C, Wrammert J, et al.
689 Induction of broadly cross-reactive antibody responses to the influenza HA stem
690 region following H5N1 vaccination in humans. *Proceedings of the National*
691 *Academy of Sciences of the United States of America.* 2014;111(36):13133-8.
692 11. Wheatley AK, Whittle JRR, Lingwood D, Kanekiyo M, Yassine HM, Ma SS,
693 et al. H5N1 Vaccine-Elicited Memory B Cells Are Genetically Constrained by
694 the IGHV Locus in the Recognition of a Neutralizing Epitope in the
695 Hemagglutinin Stem. *Journal of immunology.* 2015;195(2):602-10.
696 12. Wrammert J, Koutsonanos D, Li GM, Edupuganti S, Sui J, Morrissey M, et al.
697 Broadly cross-reactive antibodies dominate the human B cell response against
698 2009 pandemic H1N1 influenza virus infection. *The Journal of experimental*
699 *medicine.* 2011;208(1):181-93.
700 13. Andrews SF, Huang Y, Kaur K, Popova LI, Ho IY, Pauli NT, et al. Immune
701 history profoundly affects broadly protective B cell responses to influenza.
702 *Science translational medicine.* 2015;7(316).
703 14. Eggink D, Goff PH, and Palese P. Guiding the immune response against
704 influenza virus hemagglutinin toward the conserved stalk domain by
705 hyperglycosylation of the globular head domain. *Journal of virology.*
706 2014;88(1):699-704.
707 15. Angeletti D, Gibbs JS, Angel M, Kosik I, Hickman HD, Frank GM, et al.
708 Defining B cell immunodominance to viruses. *Nat Immunol.* 2017;18(4):456-
709 63.
710 16. Altman MO, Bennink JR, Yewdell JW, and Herrin BR. Lamprey VLRB
711 response to influenza virus supports universal rules of immunogenicity and
712 antigenicity. *eLife.* 2015;7(4).
713 17. Jegaskanda S, Weinfurter JT, Friedrich TC, and Kent SJ. Antibody-dependent
714 cellular cytotoxicity is associated with control of pandemic H1N1 influenza
715 virus infection of macaques. *Journal of virology.* 2013;87(10):5512-22.
716 18. Choi EY, Christianson GJ, Yoshimura Y, Sproule TJ, Jung N, Joyce S, et al.
717 Immunodominance of H60 is caused by an abnormally high precursor T cell
718 pool directed against its unique minor histocompatibility antigen peptide.
719 *Immunity.* 2002;17(5):593-603.
720 19. La Gruta NL, Kedzierska K, Pang K, Webby R, Davenport M, Chen W, et al.
721 A virus-specific CD8+ T cell immunodominance hierarchy determined by
722 antigen dose and precursor frequencies. *Proceedings of the National Academy*
723 *of Sciences of the United States of America.* 2006;103(4):994-9.
724 20. Kuraoka M, Schmidt AG, Nojima T, Feng F, Watanabe A, Kitamura D, et al.
725 Complex Antigens Drive Permissive Clonal Selection in Germinal Centers.
726 *Immunity.* 2016;44(3):542-52.
727 21. Whittle JRR, Wheatley AK, Wu L, Lingwood D, Kanekiyo M, Ma SS, et al.
728 Flow cytometry reveals that H5N1 vaccination elicits cross-reactive stem-
729 directed antibodies from multiple Ig heavy-chain lineages. *Journal of virology.*
730 2014;88(8):4047-57.
731 22. Jegaskanda S, Mason RD, Andrews SF, Wheatley AK, Zhang R, Reynoso GV,
732 et al. Intranasal Live Influenza Vaccine Priming Elicits Localized B Cell
733 Responses in Mediastinal Lymph Nodes. *Journal of virology.* 2018;92(9).
734 23. Frank GM, Angeletti D, Ince WL, Gibbs JS, Khurana S, Wheatley AK, et al. A
735 Simple Flow-Cytometric Method Measuring B Cell Surface Immunoglobulin
736 Avidity Enables Characterization of Affinity Maturation to Influenza A Virus.
737 *mBio.* 2015;6(4).
738 24. Rothaeusler K, and Baumgarth N. B-cell fate decisions following influenza
739 virus infection. *Eur J Immunol.* 2010;40(2):366-77.

740 25. Das SR, Hensley SE, Ince WL, Brooke CB, Subba A, Delboy MG, et al.
741 Defining influenza A virus hemagglutinin antigenic drift by sequential
742 monoclonal antibody selection. *Cell host & microbe.* 2013;13(3):314-23.
743 26. Lee BO, Rangel-Moreno J, Moyron-Quiroz JE, Hartson L, Makris M, Sprague
744 F, et al. CD4 T cell-independent antibody response promotes resolution of
745 primary influenza infection and helps to prevent reinfection. *J Immunol.*
746 2005;175(9):5827-38.
747 27. Mozdzanowska K, Furchner M, Zharikova D, Feng J, and Gerhard W. Roles of
748 CD4+ T-cell-independent and -dependent antibody responses in the control of
749 influenza virus infection: evidence for noncognate CD4+ T-cell activities that
750 enhance the therapeutic activity of antiviral antibodies. *Journal of virology.*
751 2005;79(10):5943-51.
752 28. Dan JM, Lindestam Arlehamn CS, Weiskopf D, da Silva Antunes R, Havenar-
753 Daughton C, Reiss SM, et al. A Cytokine-Independent Approach To Identify
754 Antigen-Specific Human Germinal Center T Follicular Helper Cells and Rare
755 Antigen-Specific CD4+ T Cells in Blood. *J Immunol.* 2016;197(3):983-93.
756 29. Havenar-Daughton C, Reiss SM, Carnathan DG, Wu JE, Kendric K, Torrents
757 de la Pena A, et al. Cytokine-Independent Detection of Antigen-Specific
758 Germinal Center T Follicular Helper Cells in Immunized Nonhuman Primates
759 Using a Live Cell Activation-Induced Marker Technique. *J Immunol.*
760 2016;197(3):994-1002.
761 30. Reiss S, Baxter AE, Cirelli KM, Dan JM, Morou A, Daigneault A, et al.
762 Comparative analysis of activation induced marker (AIM) assays for sensitive
763 identification of antigen-specific CD4 T cells. *PloS one.*
764 2017;12(10):e0186998.
765 31. Kristensen AB, Lay WN, Ana-Sosa-Batiz F, Vanderven HA, Madhavi V,
766 Laurie KL, et al. Antibody Responses with Fc-Mediated Functions after
767 Vaccination of HIV-Infected Subjects with Trivalent Influenza Vaccine.
768 *Journal of virology.* 2016;90(12):5724-34.
769 32. Valkenburg SA, Mallajosyula VV, Li OT, Chin AW, Carnell G, Temperton N,
770 et al. Stalking influenza by vaccination with pre-fusion headless HA mini-stem.
771 *Sci Rep.* 2016;6:22666.
772 33. Bommakanti G, Citron MP, Hepler RW, Callahan C, Heidecker GJ, Najar TA,
773 et al. Design of an HA2-based Escherichia coli expressed influenza immunogen
774 that protects mice from pathogenic challenge. *Proceedings of the National*
775 *Academy of Sciences.* 2010.
776 34. Mallajosyula VVA, Citron MP, Ferrara F, Lu X, Callahan C, Heidecker GJ, et
777 al. Influenza hemagglutinin stem-fragment immunogen elicits broadly
778 neutralizing antibodies and confers heterologous protection. *Proceedings of the*
779 *National Academy of Sciences.* 2014.
780 35. Steel J, Lowen AC, Wang TT, Yondola M, Gao Q, Haye K, et al. Influenza
781 virus vaccine based on the conserved hemagglutinin stalk domain. *MBio.*
782 2010;1(1).
783 36. Wohlbold TJ, Nachbagauer R, Margine I, Tan GS, Hirsh A, and Krammer F.
784 Vaccination with soluble headless hemagglutinin protects mice from challenge
785 with divergent influenza viruses. *Vaccine.* 2015;33(29):3314-21.
786 37. Bodewes R, de Mutsert G, van der Klis FR, Ventresca M, Wilks S, Smith DJ,
787 et al. Prevalence of antibodies against seasonal influenza A and B viruses in
788 children in Netherlands. *Clinical and vaccine immunology : CVI.*
789 2011;18(3):469-76.

790 38. Kucharski AJ, Lessler J, Read JM, Zhu H, Jiang CQ, Guan Y, et al. Estimating
791 the life course of influenza A(H3N2) antibody responses from cross-sectional
792 data. *PLoS biology.* 2015;13(3).
793 39. Li GM, Chiu C, Wrammert J, McCausland M, Andrews SF, Zheng NY, et al.
794 Pandemic H1N1 influenza vaccine induces a recall response in humans that
795 favors broadly cross-reactive memory B cells. *Proceedings of the National*
796 *Academy of Sciences of the United States of America.* 2012;109(23):9047-52.
797 40. Krammer F. Novel universal influenza virus vaccine approaches. *Curr Opin*
798 *Virol.* 2016;17:95-103.
799 41. Krammer F, Hai R, Yondola M, Tan GS, Leyva-Grado VH, Ryder AB, et al.
800 Assessment of influenza virus hemagglutinin stalk-based immunity in ferrets.
801 *Journal of virology.* 2014;88(6):3432-42.
802 42. Krammer F, Pica N, Hai R, Margine I, and Palese P. Chimeric hemagglutinin
803 influenza virus vaccine constructs elicit broadly protective stalk-specific
804 antibodies. *Journal of virology.* 2013;87(12):6542-50.
805 43. Okuno Y, Isegawa Y, Sasao F, and Ueda S. A common neutralizing epitope
806 conserved between the hemagglutinins of influenza A virus H1 and H2 strains.
807 *Journal of virology.* 1993;67(5):2552-8.
808 44. Bodewes R, Geelhoed-Mieras MM, Wrammert J, Ahmed R, Wilson PC,
809 Fouchier RA, et al. In vitro assessment of the immunological significance of a
810 human monoclonal antibody directed to the influenza a virus nucleoprotein.
811 *Clin Vaccine Immunol.* 2013;20(8):1333-7.
812 45. Wu X, Yang ZY, Li Y, Hogerkorp CM, Schief WR, Seaman MS, et al. Rational
813 design of envelope identifies broadly neutralizing human monoclonal
814 antibodies to HIV-1. *Science.* 2010;329(5993):856-61.
815 46. van Baalen CA, Jeeninga RE, Penders GH, van Gent B, van Beek R, Koopmans
816 MP, et al. ViroSpot microneutralization assay for antigenic characterization of
817 human influenza viruses. *Vaccine.* 2017;35(1):46-52.
818

819

820 # Figure Legends

821 **Figure 1. Serological and B cell responses in experimentally infected mice**

822 (A) Serum endpoint total IgG titres were measured by ELISA using HA-FL (blue) or
823 stabilised HA-stem (red) in mice infected intranasally with A/Puerto Rico/08/1934 (n
824 = 6 per timepoint). Dotted lines denote detection cut off (1:100 dilution). Data represent
825 mean ± SEM. (B) Frequency of GC (B220+/IgD-/CD38lo/GL7+) and memory B cells
826 (B220+/IgD-/CD38hi/GL7-) binding HA-FL (blue) or HA-stem (red) (n = 6). Data
827 represent mean ± SEM. (C) Frequency of plasma cells (CD138+B220-IgD-) binding
828 HA-FL (blue) or HA-stem (red) (n = 6). Data represent mean ± SEM. (D) HA
829 bioavailability visualised by monoclonal anti-HA head or stem antibody staining
830 (white) and B220+ B cells staining (green); scale bar - 100 μM.

831

832 **Figure 2. Serological and B cell responses in experimentally infected macaques**

833 (A) Serum endpoint total IgG titres were measured by ELISA using CA09 HA-FL
834 (blue) or stabilised CA09 HA-stem (red) in macaques (n = 8) infected intranasally with
835 A/Auckland/1/2009. Note two animals were sacrificed at d23. Dotted lines denote
836 detection cut off (dilution 1:100). (B) Frequency of IgG+ memory B cells (CD19+IgD-
837 IgG+) binding CA09 HA-FL (blue) or stabilised CA09 HA-stem (red) were measured
838 by flow cytometry within cryopreserved PBMC samples from infected macaques (n =
839 6). Note two animals sacrificed at d23 were excluded.

840

841 **Figure 3. Serological and B cell responses in primary vaccinated mice**

842 Serum endpoint total IgG titres were measured by ELISA using HA-FL, HA-stem or
843 PE proteins in mice that were (A) immunised 5 times with unadjuvanted immunogens
844 or (B) 2 times with adjuvanted (Addavax) immunogens (n = 10, two independent
845 experiments with groups of five animals). Mice were immunised at 3 week intervals

846 and serum collection was performed every 2 weeks post-immunisation. Dotted lines
847 denote detection cut off (dilution 1:400). Box boundaries represent 25th and 75th
848 percentiles, inner line represents median and whiskers represent min and max values.
849 (C) Representative flow cytometry plots and (D) frequency of GC B cells (B220+/IgD-
850 /CD38lo/GL7+) from mice vaccinated once with adjuvanted (Addavax) immunogens
851 double stained with HA-stem probes (A/Puerto Rico/08/1934) (n = 10, two independent
852 experiments with groups of five animals). Bars indicate mean ± SEM.
853
854 **Figure 4. Antigen specificity of Tfh cells following immunization or infection in**
855 **mice**
856 (A) Tfh cells were quantified in the two draining inguinal lymph nodes at day 14 post-
857 vaccination with PR8 HA-FL or stem-KLH antigens (n=5). (B-D) Antigen-specific Tfh
858 cells were identified either by OX-40 upregulation in combination with ICOS^{++} or
859 CD25 co-expression or CD154 expression following 18 hours of stimulation with HA
860 head or HA stem peptide pools. Antigen-specific responses are presented after
861 background subtraction using a DMSO control (dotted line indicates no change above
862 background). Samples were collected at day 14 post-immunization or infection with
863 PR8 HA-FL (n = 12), stem-KLH protein (n = 10), or 50 $TCID_{50}$ PR8 virus (n = 5). Bars
864 indicate median and interquartile range. Statistics assessed by Wilcoxon matched-pairs
865 test; **P < 0.01.
866
867 **Figure 5. Stem immunogens fail to selectively recall stem antibody in pre-immune**
868 **mice and macaques**
869 Mice infected intranasally with A/Puerto Rico/08/1934 and immunised at day 56 were
870 analysed for (A) serum endpoint total IgG titres measured by ELISA at day 56 (black
871 box – pre-immunisation) and day 70 (white box – 2 weeks post-immunisation) using

872 HA-FL or HA-stem proteins (n = 10, two independent experiments with groups of five
873 animals), and (B) frequency of GC B cells (B220+/IgD-/CD38lo/GL7+) stained with
874 HA-FL and HA-stem probes (A/Puerto Rico/08/1934) measured by flow cytometry (n
875 = 5). Box boundaries represent 25th and 75th percentiles, inner line represents median
876 and whiskers represent min and max values. Bars indicate mean ± SEM. Results
877 compared with Mann-Whitney U; *P < 0.05. Macaques (n = 6) infected intranasally
878 with A/Auckland/1/2009 and immunised at day 56 with seasonal quadrivalent
879 inactivated influenza vaccine (IIV4) or HA-stem immunogen were analysed for (C)
880 serum endpoint total IgG titres measured by ELISA using CA09 HA-FL (blue) or
881 stabilised CA09 HA-stem (red) proteins, and (D) frequency of IgG+ memory B cells
882 (CD19+IgD-IgG+) binding CA09 HA-FL (blue) or stabilised CA09 HA-stem (red)
883 probes measured by flow cytometry within cryopreserved PBMC samples. Dotted lines
884 denote detection cut off (dilution 1:100).
885
886 **Figure 6. Stem antibody and memory B cells are expanded by seasonal influenza**
887 **vaccination in humans**
888 (A) Serum endpoint total IgG titres of antibody binding the HA-FL (blue) or the
889 stabilised HA-stem domain (red) at baseline and following immunisation (day 28) with
890 seasonal IIV3 (n = 29) or IIV4 (2016 – n = 18; 2017 – n = 21). Results compared with
891 Mann-Whitney U; *P < 0.05. (B) Representative flow cytometry plots of IgG+ memory
892 B cells from IIV4 (2016) recipients double stained with recombinant HA-FL or HA-
893 stem probes (A/California/04/2009). Memory B cells were defined as CD19+IgD-IgG+
894 after prior exclusion of doublets, dead cells and CD3+, CD14+, CD16+, CD8+ and
895 CD10+ cells. The frequency (C) and percentage change (D) of IgG+ memory B cells
896 binding HA-FL or HA-stem between baseline and following IIV4 (2016) immunisation
897 (n = 18). Data represent mean ± SEM. Results compared with Mann-Whitney U; *P <

898 0.05. (E) Representative flow cytometry plots of IgG+ memory B cells from IIV4
899 (2017) recipients co-stained with recombinant HA-FL (A/Michigan/45/2015) or HA-
900 stem probes (A/California/04/2009). The frequency (F) and percentage change (G) of
901 IgG+ memory B cells binding either HA-FL or HA-stem between baseline and
902 following IIV4 (2017) immunisation (n = 21). Data represent mean ± SEM. Results
903 compared with Mann-Whitney U; *P < 0.05.

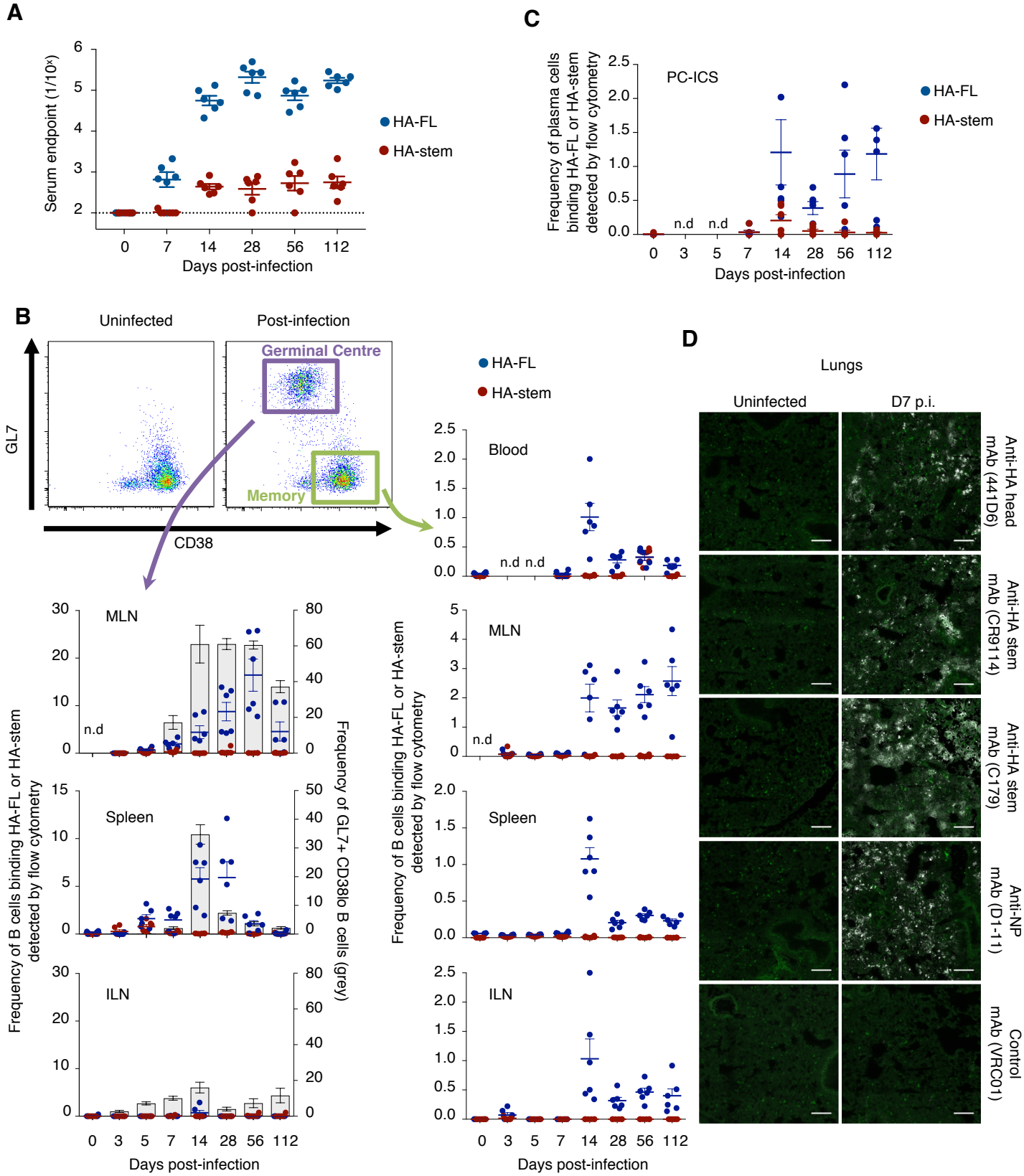

Figure 1. Serological and B cell responses in experimentally infected mice

(A) Serum endpoint total IgG titres were measured by ELISA using HA-FL (blue) or stabilised HA-stem (red) in mice infected intranasally with A/Puerto Rico/08/1934 (n = 6 per timepoint). Dotted lines denote detection cut off (1:100 dilution). Data represent mean ± SEM. **(B)** Frequency of GC (B220+/IgD-/CD38lo/GL7+) and memory B cells (B220+/IgD-/CD38hi/GL7-) binding HA-FL (blue) or HA-stem (red) (n = 6). Data represent mean ± SEM. **(C)** Frequency of plasma cells (CD138+B220-IgD-) binding HA-FL (blue) or HA-stem (red) (n = 6). Data represent mean ± SEM. **(D)** HA bioavailability visualised by monoclonal anti-HA head or stem antibody staining (white) and B220+ B cells staining (green); scale bar - 100 μM.

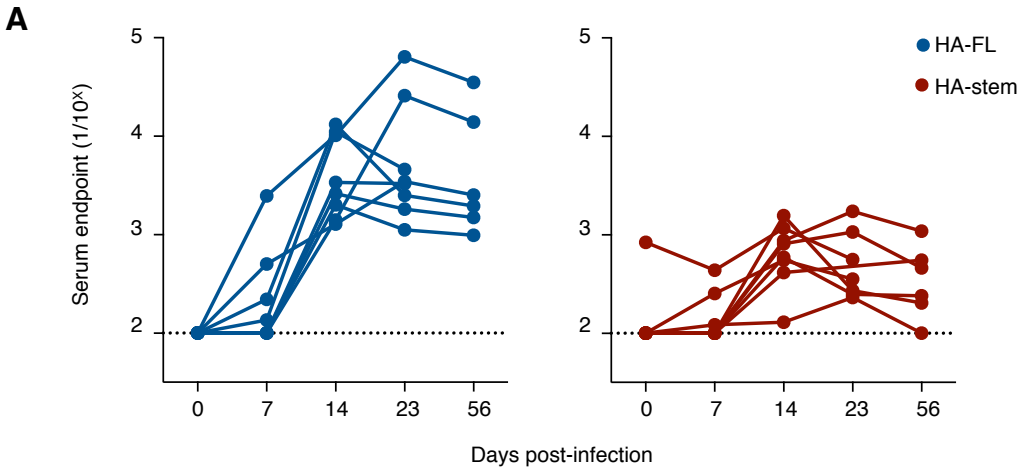

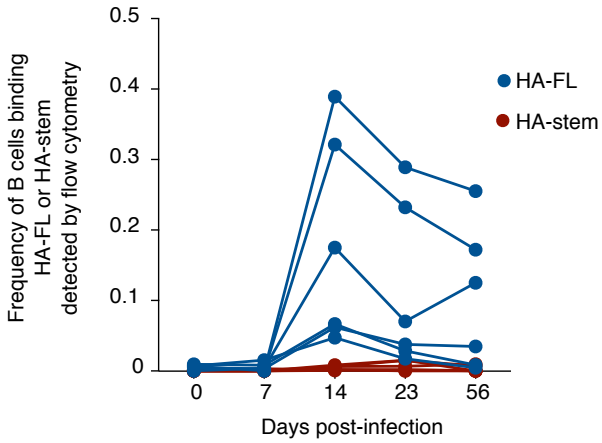

Figure 2. Serological and B cell responses in experimentally infected macaques
(A) Serum endpoint total IgG titres were measured by ELISA using CA09 HA-FL (blue) or stabilised CA09 HA-stem (red) in macaques (n = 8) infected intranasally with A/Auckland/1/2009. Note two animals were sacrificed at d23. Dotted lines denote detection cut off (dilution 1:100). **(B)** Frequency of IgG+ memory B cells (CD19+IgD-IgG+) binding CA09 HA-FL (blue) or stabilised CA09 HA-stem (red) were measured by flow cytometry within cryopreserved PBMC samples from infected macaques (n = 6). Note two animals sacrificed at d23 were excluded.

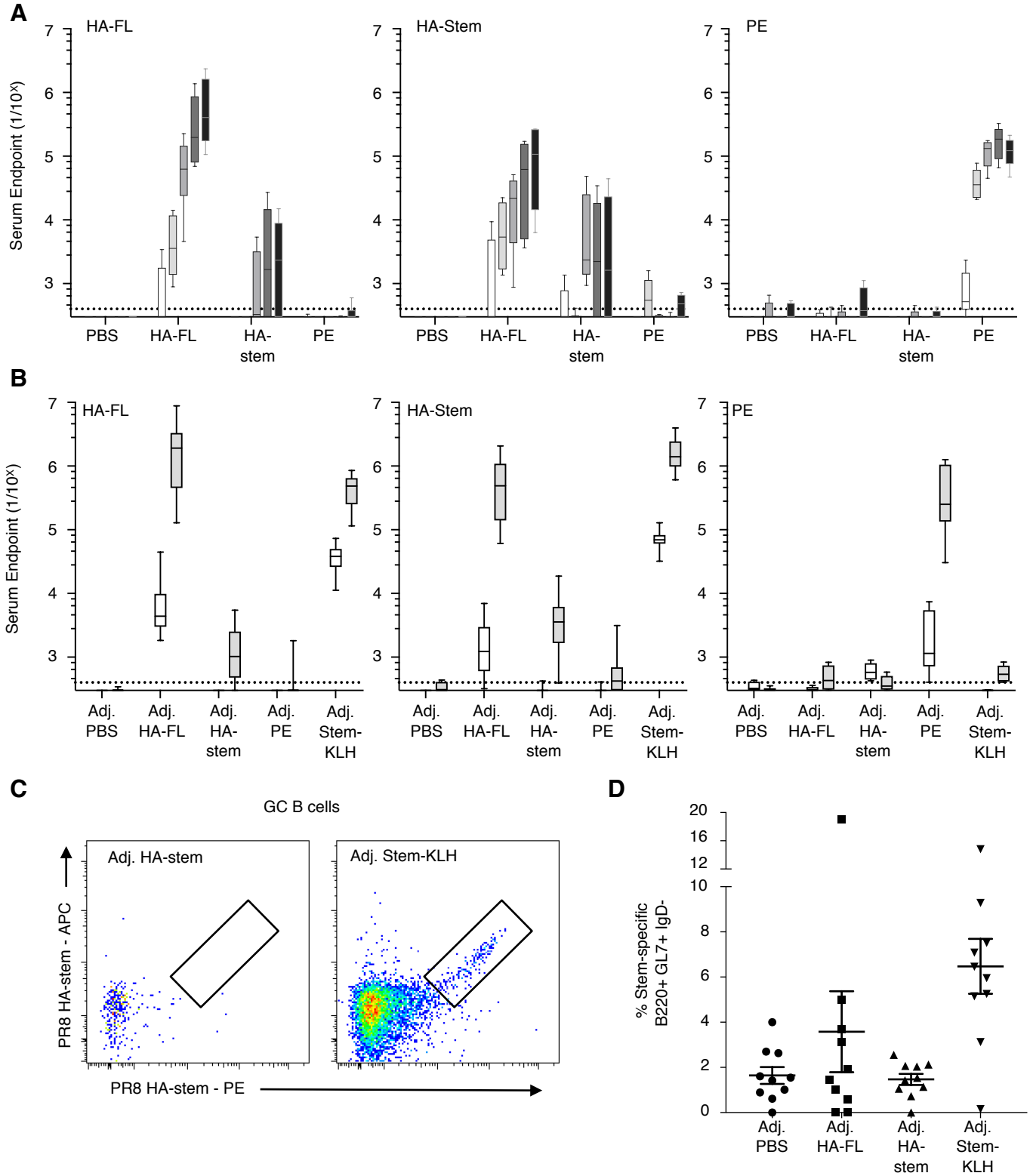

Figure 3. Serological and B cell responses in primary vaccinated mice

Serum endpoint total IgG titres were measured by ELISA using HA-FL, HA-stem or PE proteins in mice that were **(A)** immunised 5 times with unadjuvanted immunogens or **(B)** 2 times with adjuvanted (Addavax) immunogens (n = 10, two independent experiments with groups of five animals). Mice were immunised at 3 week intervals and serum collection was performed every 2 weeks post-immunisation. Dotted lines denote detection cut off (dilution 1:400). Box boundaries represent 25th and 75th percentiles, inner line represents median and whiskers represent min and max values. **(C)** Representative flow cytometry plots and **(D)** frequency of GC B cells (B220+/IgD-/CD38lo/GL7+) from mice vaccinated once with adjuvanted (Addavax) immunogens double stained with HA-stem probes (A/Puerto Rico/08/1934) (n = 10, two independent experiments with groups of five animals). Bars indicate mean ± SEM.

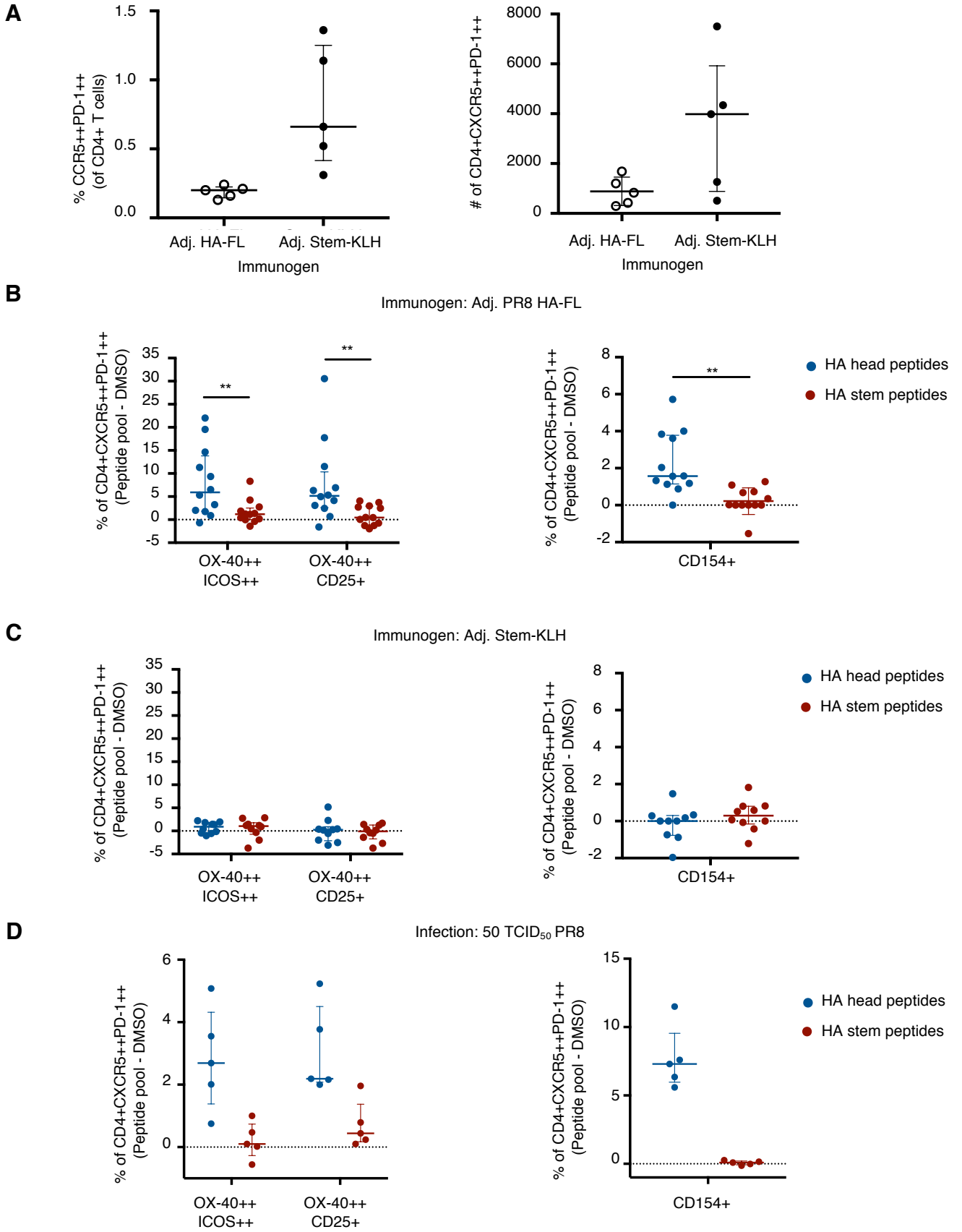

Figure 4. Antigen specificity of Tfh cells following immunization or infection in mice

(A) Tfh cells were quantified in the two draining inguinal lymph nodes at day 14 post-vaccination with PR8 HA-FL or stem-KLH antigens (n=5). **(B-D)** Antigen-specific Tfh cells were identified either by OX-40 upregulation in combination with ICOS^{++} or CD25 co-expression or CD154 expression following 18 hours of stimulation with HA head or HA stem peptide pools. Antigen-specific responses are presented after background subtraction using a DMSO control (dotted line indicates no change above background). Samples were collected at day 14 post-immunization or infection with PR8 HA-FL (n = 12), stem-KLH protein (n = 10), or 50 $TCID_{50}$ PR8 virus (n = 5). Bars indicate median and interquartile range. Statistics assessed by Wilcoxon matched-pairs test; **$P < 0.01$.

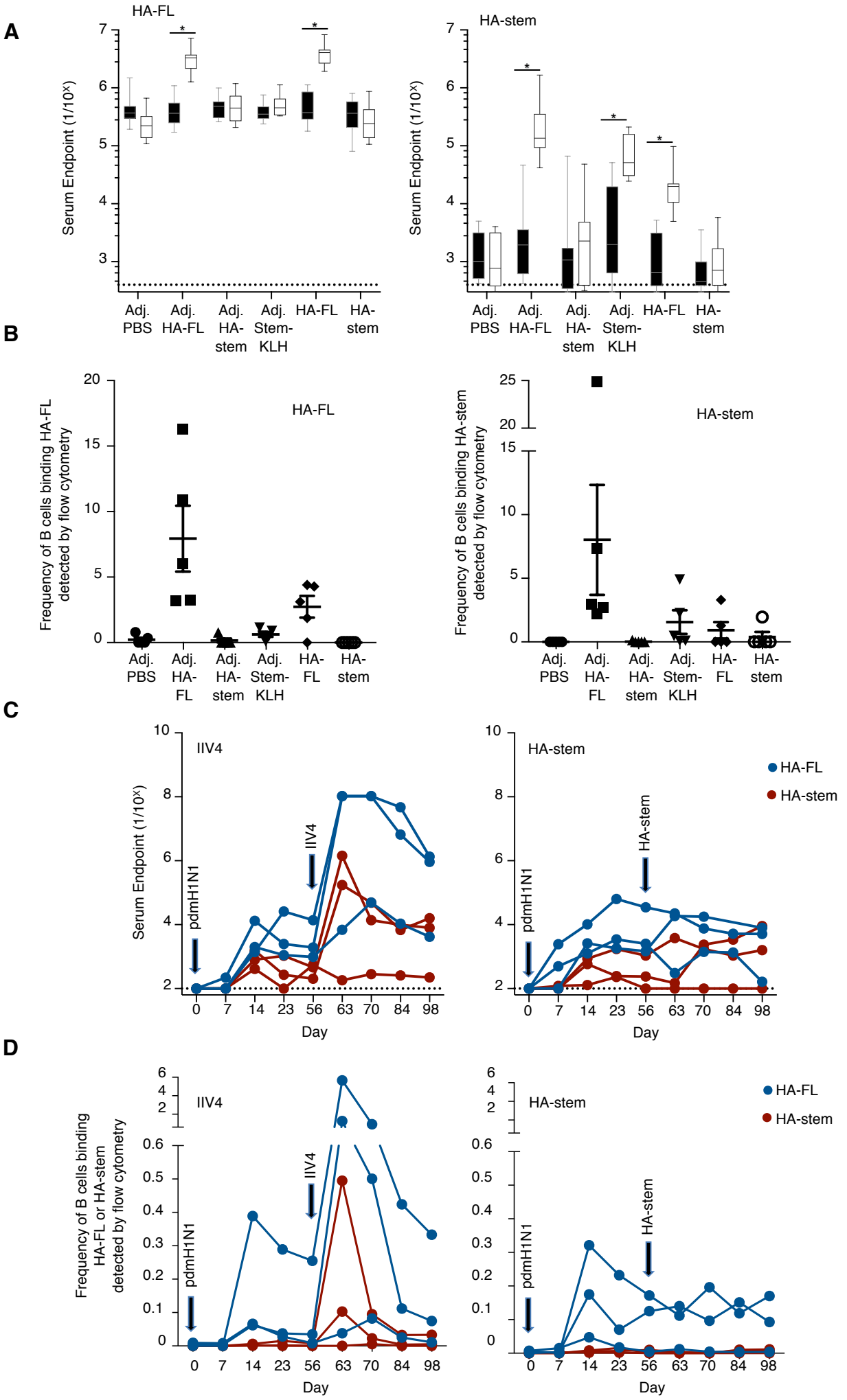
A
HA-FL
HA-stem
Serum Endpoint (1/10^X)
Adj. PBS
Adj. HA-FL
Adj. HA-stem
Adj. Stem-KLH
HA-FL
HA-stem
B
Frequency of B cells binding HA-FL detected by flow cytometry
Frequency of B cells binding HA-stem detected by flow cytometry
C
IIV4
HA-stem
HA-FL
pdmH1N1
Day
D
Frequency of B cells binding HA-FL or HA-stem detected by flow cytometry

Figure 5. Stem immunogens fail to selectively recall stem antibody in pre-immune mice and macaques
Mice infected intranasally with A/Puerto Rico/08/1934 and immunised at day 56 were analysed for **(A)** serum endpoint total IgG titres measured by ELISA at day 56 (black box – pre-immunisation) and day 70 (white box – 2 weeks post-immunisation) using HA-FL or HA-stem proteins (n = 10, two independent experiments with groups of five animals), and **(B)** frequency of GC B cells (B220+/IgD-/CD38lo/GL7+) stained with HA-FL and HA-stem probes (A/Puerto Rico/08/1934) measured by flow cytometry (n = 5). Box boundaries represent 25th and 75th percentiles, inner line represents median and whiskers represent min and max values. Bars indicate mean ± SEM. Results compared with Mann-Whitney U; *$P < 0.05$. Macaques (n = 6) infected intranasally with A/Auckland/1/2009 and immunised at day 56 with seasonal quadrivalent inactivated influenza vaccine (IIV4) or HA-stem immunogen were analysed for **(C)** serum endpoint total IgG titres measured by ELISA using CA09 HA-FL (blue) or stabilised CA09 HA-stem (red) proteins, and **(D)** frequency of IgG+ memory B cells (CD19+IgD-IgG+) binding CA09 HA-FL (blue) or stabilised CA09 HA-stem (red) probes measured by flow cytometry within cryopreserved PBMC samples. Dotted lines denote detection cut off (dilution 1:100).

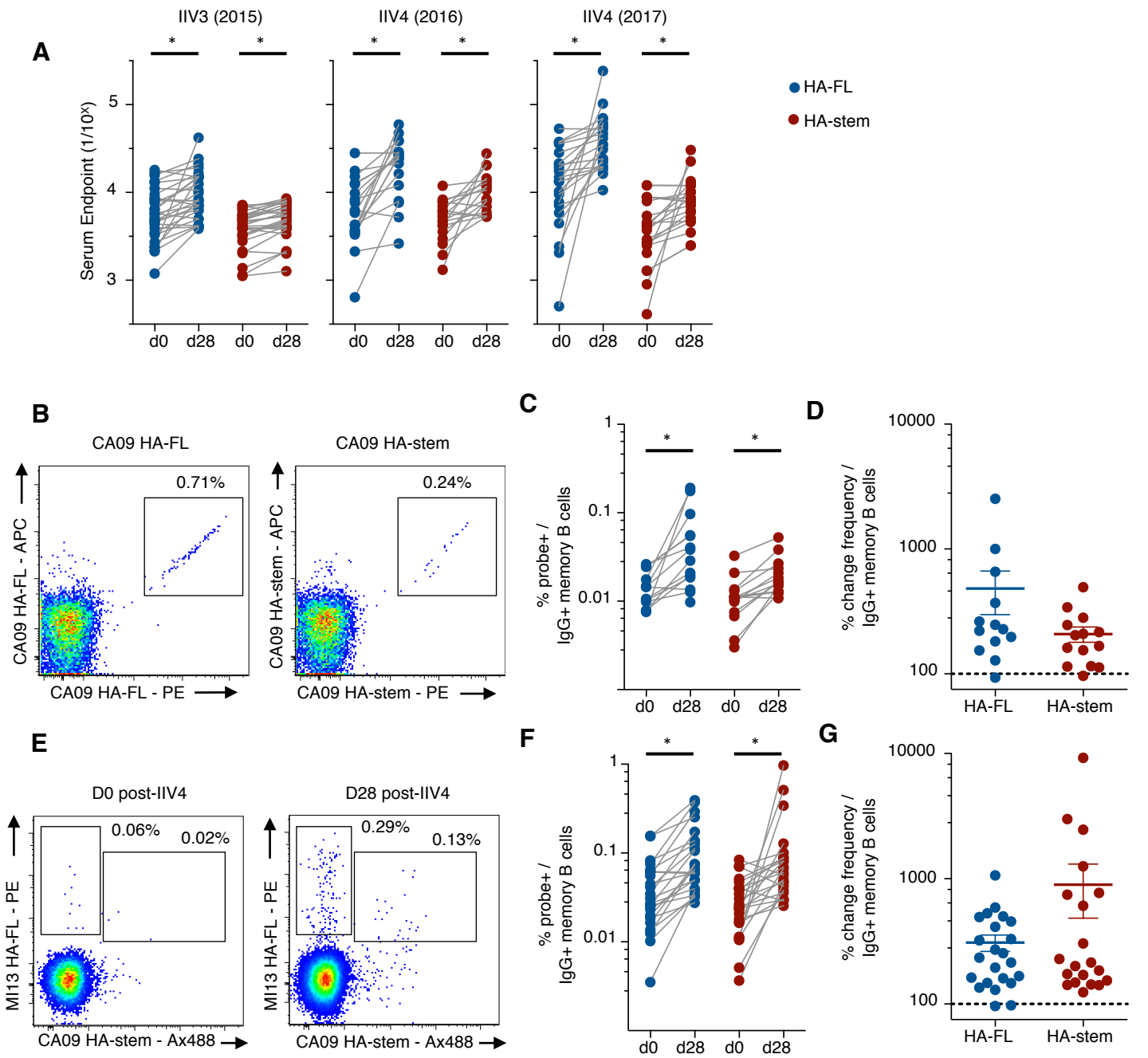

Figure 6. Stem antibody and memory B cells are expanded by seasonal influenza vaccination in humans

(A) Serum endpoint total IgG titres of antibody binding the HA-FL (blue) or the stabilised HA-stem domain (red) at baseline and following immunisation (day 28) with seasonal IIV3 (n = 29) or IIV4 (2016 – n = 18; 2017 – n = 21). Results compared with Mann-Whitney U; *P < 0.05. **(B)** Representative flow cytometry plots of IgG+ memory B cells from IIV4 (2016) recipients double stained with recombinant HA-FL or HA-stem probes (A/California/04/2009). Memory B cells were defined as CD19+IgD-IgG+ after prior exclusion of doublets, dead cells and CD3+, CD14+, CD16+, CD8+ and CD10+ cells. The frequency **(C)** and percentage change **(D)** of IgG+ memory B cells binding HA-FL or HA-stem between baseline and following IIV4 (2016) immunisation (n = 18). Data represent mean ± SEM. Results compared with Mann-Whitney U; *P < 0.05. **(E)** Representative flow cytometry plots of IgG+ memory B cells from IIV4 (2017) recipients co-stained with recombinant HA-FL (A/Michigan/45/2015) or HA-stem probes (A/California/04/2009). The frequency **(F)** and percentage change **(G)** of IgG+ memory B cells binding either HA-FL or HA-stem between baseline and following IIV4 (2017) immunisation (n = 21). Data represent mean ± SEM. Results compared with Mann-Whitney U; *P < 0.05.